Nanotechnology **18** (2007) 255701 (5pp) doi:10.1088/0957-4484/18/25/255701

Radio-frequency transmission characteristics of a multi-walled carbon nanotube

Seong Chan Jun[1], J H Choi[2], S N Cha[1], C W Baik[1], Sanghyo Lee[3], H Jin Kim[4], James Hone[5] and J M Kim[1]

[1] Display Device and Material Laboratory, Samsung Advanced Institute of Technology, Mt. 14-1, Nongseo-Dong, Giheung-Gu, Yongin-Si, Gyeonggi-Do, 449-712, Korea
[2] Communication and Connectivity Laboratory, Samsung Advanced Institute of Technology, Mt. 14-1, Nongseo-Dong, Giheung-Gu, Yongin-Si, Gyeonggi-Do, 449-712, Korea
[3] School of Electrical Engineering and Computer Sciences, Seoul National University, Seoul, 151-742, Korea
[4] School of Mechanical and Aerospace Engineering, Seoul National University, Seoul, 151-742, Korea
[5] Department of Mechanical Engineering and Nanoscale Science and Engineering Center, Columbia University, New York, NY 10027, USA

E-mail: hjinkim@snu.ac.kr and jongkim@samsung.com

Received 8 February 2007, in final form 21 April 2007
Published 29 May 2007
Online at stacks.iop.org/Nano/18/255701

Abstract
Carbon nanotubes (CNTs) are considered as promising candidates for transmission lines as well as microcircuit interconnects in future nanoscale electronic systems. Owing to the growing interest in the use of microwave signals, understanding the transmission properties at high frequencies is essential to assess the applicability of multi-walled carbon nanotubes (MWNTs). In this work, we measured two-port properties of individual MWNTs using a network analyser from a frequency of 0.5 to 50 GHz. The radio-frequency transmission parameters were obtained from the measured S-parameter data. Our results show the frequency dependence of the equivalent resistance of MWNTs, which decreases with increasing frequency. This confirms that metallic CNTs will be useful for transmitting GHz signals in nanoelectric devices.

(Some figures in this article are in colour only in the electronic version)

1. Introduction

In recent years carbon nanotubes (CNTs) have emerged as promising candidates to solve the issue of limited transportation capacity of thin metal wires due to signal loss and scattering in nanosized electronic components. The material properties of CNTs can rival or even exceed those of known materials in the case of interconnectors, semiconductors, and field emission devices. With growing interest in the use of gigahertz and terahertz regimes, understanding the transmission characteristics of CNTs is especially valuable.

Since the discovery of CNTs, their electrical properties have been actively studied and they are being used in nanoscale circuits [1–3]. However, most of the known transport properties of CNTs are their DC properties, such as DC resistance, or the effect of gate bias voltage or temperature on the resistance. There has been some recent research on the radio-frequency (RF) characterization of single-walled nanotubes (SWNTs). An RF model for metallic SWNTs was suggested [4], and from a theoretical point of view, the microwave passive [5] and active [6] electrical properties of CNTs were analysed. In addition, SWNT transistors with high Q-factors have been fabricated [7, 8]. However, theoretical predictions that the AC transport will be qualitatively different from DC transport [9–13] have not been fully confirmed. For example, one-port measurements of a single metallic SWNT

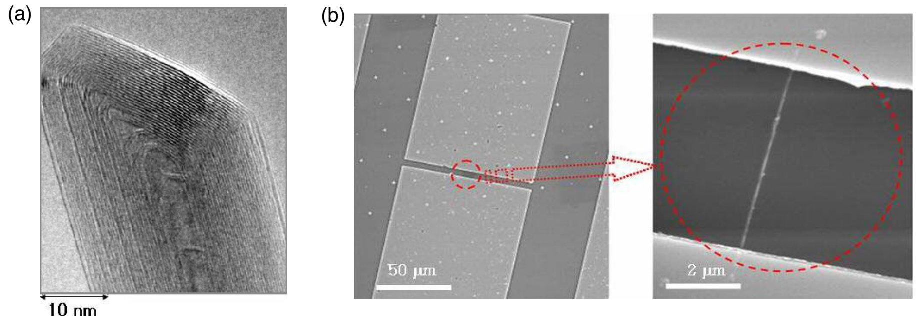

Figure 1. (a) TEM image of one of the MWNTs selected for the experiments. (b) An SEM image of the IN/OUT electrode part of the sample. The close-up view shows that the IN and OUT electrodes for GSG measurements are connected by a single MWNT.

up to 10 GHz [14], and a SWNT field-effect transistor at 1 GHz [8], did not reveal frequency dependence of the CNT dynamic impedance. On the other hand, frequency-dependent impedance of a semiconducting SWNT was reported up to 8 MHz [15]. In addition, in a two-port experiment using a bundle of SWNTs rather than a single SWNT, the overall resistance of the SWNT bundle decreased as frequency increased up to 20 GHz [16]. The previous measurements are limited to a relatively low frequency range or a bundle of SWNTs, so it is difficult to derive the transmission properties of individual CNTs in the higher frequency regime.

Multi-walled nanotubes (MWNTs) are highlighted as interconnection or transmission lines for signal propagation, because of their metallic properties and multi-layered structure leading to a lower resistance than typical SWNTs. However, much less is known about the electric transmission characteristics of MWNTs. Recently, frequency-dependent impedance up to 200 kHz was reported from a MWNT with very narrow electrode gaps of 0.05–1 μm [17]. With such narrow gaps, parasitic effects from electrodes and contacts become too profound to observe the intrinsic properties, and the measured frequency range is rather limited. To our knowledge, microwave transmission properties of MWNTs have not been measured previously, and parametrization with circuit elements has not been performed. In this paper, we characterized the microwave transmission characteristics of individual MWNTs by measuring S-parameters in a two-port experiment from 0.5 to 50 GHz, and extracting frequency-dependent equivalent transmission line parameters from the data.

2. Experimental details

2.1. Sample fabrication

MWNTs grown by a plasma-enhanced chemical-vapour deposition technique (PECVD) were placed in ethanol solvent. This solution was sonicated and spin-coated on a 150 nm SiO_2 film substrate. Randomly scattered MWNTs were examined using SEM, and CNTs of approximately 25 nm in diameter and 7 μm in length, as shown in figure 1(a), were selected. The metal pads, designed to be compatible with the ground–signal–ground (GSG) probes, consisted of two 250 μm $\times$ 250 μm contact pads for ground, and IN and OUT electrodes. The metal electrodes were formed using Nb (150 nm). In order to reduce contact resistance, the deposition rate of Nb by the thermal evaporator was set to as low as 0.8 nm min^{-1}. Figure 1(b) shows the MWNT connecting the IN and OUT electrodes. The gap between the electrodes is 5 μm. For the ohmic contact formation between the CNT and the metal electrodes, thermal annealing was executed twice at 500 °C for 30 min. After the first annealing, the resistance of the prepared samples was estimated to be 73–75 kΩ, which decreased to 50–53 kΩ after the second annealing.

In addition, open devices (the same electrode pattern with no MWNT) and short devices (with lumped IN/OUT electrodes) were fabricated simultaneously with the samples with MWNTs, to de-embed the parasitic effects from the measured S-parameter data.

2.2. Measurements

The conceptual top-down view of the two-port S-parameter measurement set-up [16] is shown in figure 2(a). We measured S-parameters S_{11} and S_{12} using the network analyser HP8510XF at an RF power of -18 dB m, which sends a microwave signal from port 1 and then observes the signal wave both at port 1 and port 2. These S-parameters (or scattering matrices), obtained from these incident and reflected voltages at each frequency, provide a complete description of the network as seen at two ports. One obstacle for RF measurement of a CNT is the low current from a single CNT. There are also various factors that corrupt the S-parameter data, such as bad contacts between sample and electrodes, equipment-based resonances, and external noise. These concerns were kept in mind during the experiments, and care was exercised for the calibration and maintenance of consistent probe contact force and contact position for all sample patterns.

3. Transmission line analysis

3.1. Transmission line model

Classical RF interconnections are described by the telegrapher's transmission line model, consisting of a short two-wire line segment as shown in figure 2(b). R represents the series resistance per unit length; L represents the total self-inductance of the two conductors per unit length; the shunt capacitance per unit length C is due to the finite of the two conductors, and

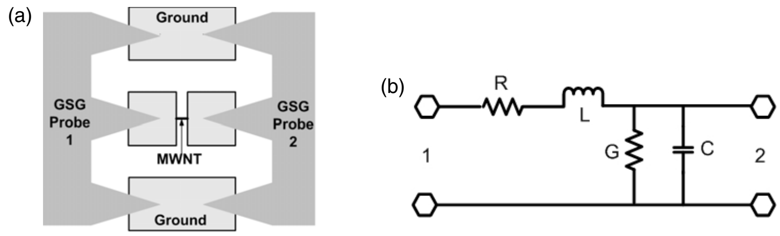

Figure 2. (a) Set-up for the two-port measurement of MWNT properties. The device consists of two ground pads, and IN and OUT electrodes that are connected by a single MWNT. (b) Equivalent circuit model for a transmission line, consisting of series resistance R, inductance L, capacitance C, and dielectric loss G.

the shunt conductance G represents dielectric loss in the material between the conductors per unit length. These distributed transmission parameters (R, L, G and C) explain the RF signal propagation constant and the characteristic impedance in the frequency domain. Once they are known in the frequency domain, we can predict the signal waveform after propagating the transmission line. One advantage of this model is that the RF transmission of the MWNT is simplified using the unit-length quantities, so this model can be easily plugged into commercial RF circuit simulators such as SPICE or ADS. It is noted that this model does not separate the contact resistance from the inherent CNT resistance.

Wave equations for travelling voltage and current for this equivalent circuit model yield the following expressions for the propagation constant γ and characteristic impedance Z as a function of frequency ω (rad s^{-1}) [20].

$$\gamma = \alpha + j\beta = \sqrt{(R + j\omega L)(G + j\omega C)} \qquad (1)$$

$$Z = \sqrt{\frac{R + j\omega L}{G + j\omega C}}. \qquad (2)$$

If γ and Z are known, the R, L, G and C values can be obtained by combining (1) and (2) as follows:

$$\begin{aligned} R &= \mathrm{Re}\{\gamma Z\} \\ L &= \mathrm{Im}\{\gamma Z\}/\omega \\ G &= \mathrm{Re}\{\gamma / Z\} \\ C &= \mathrm{Im}\{\gamma / Z\}/\omega. \end{aligned} \qquad (3)$$

3.2. S-parameter characterization

From the measured S-parameter data, the wave propagation constant γ and impedance Z can be extracted using the theory presented in [18–20]. First, the devices are considered as a symmetric two-port network so that $S_{11} = S_{22}$ and $S_{21} = S_{12}$, and the S-parameter data are converted to the following ABCD matrix, where Z_0 denotes the load for GSG probing (50 Ω):

$$\begin{bmatrix} A & B \\ C & D \end{bmatrix} = \frac{1}{2S_{21}} \times \begin{bmatrix} (1 - S_{11}^2 + S_{21}^2) & Z_0((1 + S_{11})^2 - S_{21}^2) \\ \frac{1}{Z_0}((1 - S_{11})^2 - S_{21}^2) & (1 - S_{11}^2 + S_{21}^2) \end{bmatrix}.$$

Then the propagation constant and characteristic impedance are extracted using the following relationship for a lossy transmission line:

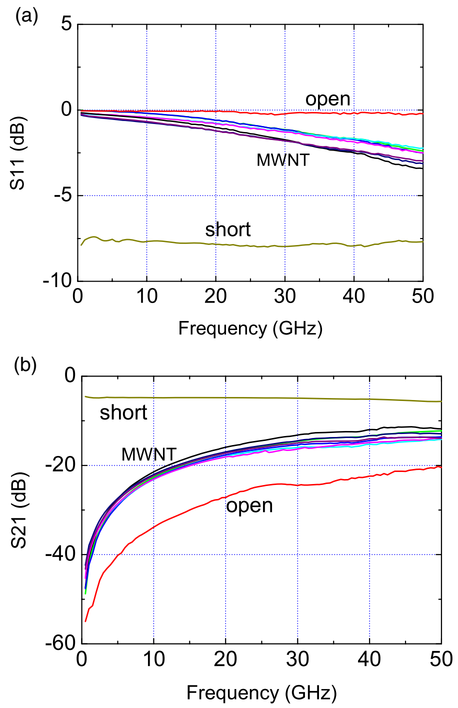

Figure 3. S-parameter data of samples with/without MWNTs, and a short sample measured from 0.5 to 50 GHz. (a) Amplitude of S_{11} in dB, and (b) S_{21} in dB.

$$\gamma = \cosh^{-1} A$$

$$Z = \sqrt{B/C}.$$

Now (3) can be used to obtain the R, L, G and C values over the measured frequency range.

4. Results and discussion

Figure 3(a) shows the amplitude of the S_{11} data obtained from the seven samples measured from 0.5 to 50 GHz, and figure 3(b) shows S_{21}. For comparison, the measurements of the open and short samples are also displayed. By comparing the data from the open and short samples, we can see that the effect of the metal pads themselves is mainly resistive, and that the very small gap between the electrodes causes a capacitive effect. The difference between the S_{21} magnitudes of the samples with and without a MWNT decreases from 12–13 dB at a few gigahertz to less than 7 dB at 50 GHz,

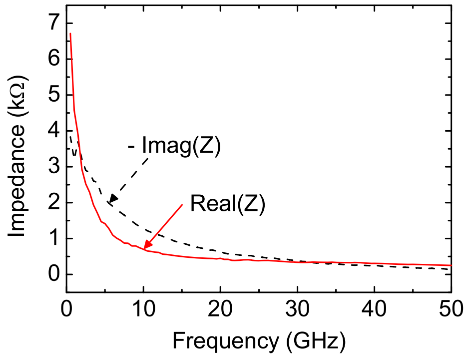

Figure 4. Real and imaginary parts of the MWNT dynamic impedance Z with respect to the frequency from 0.5 to 50 GHz.

due to the increasing parasitic capacitive contribution parallel with the device. But this difference remains large enough to be meaningful throughout the measured frequency range, which indicates that the MWNT transmits a much larger signal than the open samples.

By using the standard passive de-embedding in order to subtract parasitic effects from the MWNT data and then applying the process described in section 3, the dynamic impedance was computed. Figure 4 shows the magnitude of the real and imaginary parts of MWNT dynamic impedance as a function of frequency, obtained from the averaged data. The magnitude of both the real and imaginary parts decreases, and the magnitude of the impedance monotonically decreases from 7730 Ω at 0.5 GHz to 288 Ω at 50 GHz. The imaginary part remains negative, which means $RC > LG$ according to (2), i.e. the MWNT impedance displays a capacitive character.

Note that the total contribution to the transmission is not only from the CNT itself, but the entire impedance contributes. At high frequency, both the capacitance of the CNT and the parasitic capacitance between the IN/OUT electrodes contribute to the transmission. The capacitive coupling between the MWNTs and the electrodes also contributes to the transmission. In fact, all theoretical work [9–12] predicted that AC transport characteristics will be qualitatively different from DC transport in nanoelectric systems, in the absence of contact resistance and scattering. In addition, the quantum point contact was predicted to be significantly dependent on frequency [13]. However, it is not yet known how much the contact resistance and scattering affect the microwave transmission for CNTs. The contact resistance itself may contain both real and imaginary parts (i.e. capacitive or inductive elements), and the effect of AC on those has not been quantified clearly. Thus, it is difficult to say what portion of the value given in figure 4 represents the inherent MWNT character. However, this information indicates that the MWNT is a promising material for high-frequency transmission lines.

Figures 5(a)–(d) show R, L, G and C values extracted as described in section 3. The series resistive component R includes the effects of both the contact resistance and the inherent resistance of the CNT, and therefore has a relatively large magnitude. As plotted in figure 5(a) the resistance substantially decreases from 2.1 kΩ μm^{-1} at 0.5 GHz to 0.1 kΩ μm^{-1} at 10 GHz, and then gradually decreases to 0.05 kΩ μm^{-1} at 50 GHz. If the diameter of the metal wires is of the order of the mean free path (for example, 40 nm for Cu at room temperature), it is known that the resistance will significantly increase due to scattering [21]. Furthermore, at such small dimensions, their reduced current-carrying capacity will be worsened by joule heating and electromigration. Therefore, this reduction in the MWNT resistance with frequency is noteworthy and highly desirable in transmitting very high-frequency currents.

Figure 5(b) shows that the series inductance decreases from 215 to 0.02 μH μm^{-1} as frequency increases from 0.5 to 50 GHz. It decreases significantly up to 10 GHz

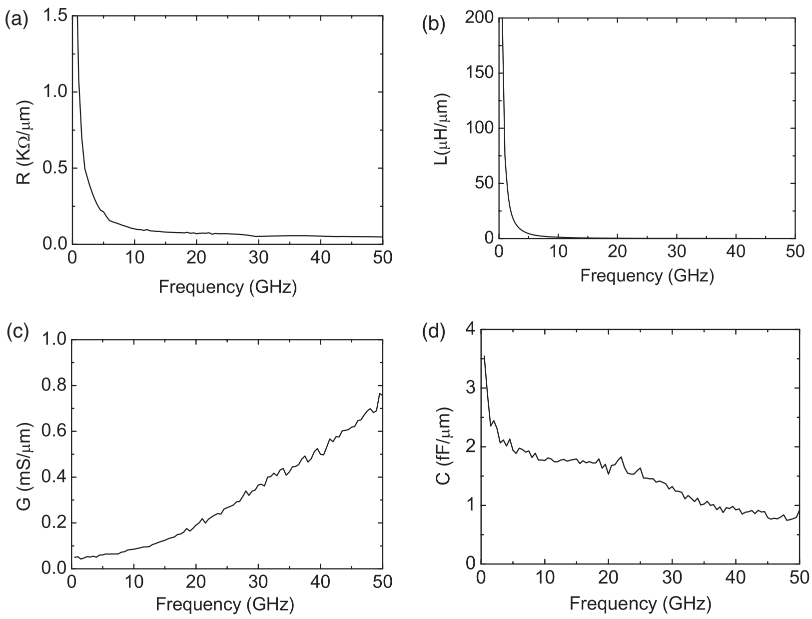

Figure 5. Equivalent transmission line parameters extracted from the averaged measured data with respect to the frequency. (a) Resistance per unit length, (b) inductance per unit length, (c) shunt capacitance per unit length, and (d) capacitance per unit length.

and then remains relatively constant. Figure 5(c) shows that G increases monotonically from 0.05 to 0.75 mS μm^{-1}. It is usually assumed that dielectric loss is negligible, but significant conductive dielectric loss is suggested at microwave frequencies. One reason behind the frequency-dependent inductance and shunt conductance could be the so-called substrate skin effect [22], where the time-varying magnetic flux penetrating into the silicon substrate leads to frequency-dependent fields. This results in frequency-dependent eddy currents in the substrate, which can cause a significant reduction in inductance and a significant increase in loss. In figure 5(d), the capacitance C gradually decreases from 3.5 to 0.9 fF μm^{-1}. However, it should be noted that the effect of a constant value of inductance or capacitance on signal propagation is proportional to frequency as in (1).

Given that a one-port measurement of a SWNT did not reveal a frequency dependence [14], whereas the overall resistance decreased in two-port experiments of a bundle of SWNTs [16], it is possible that the high resistance of SWNTs causes significant difficulty in analysing the SWNT RF characteristics. Because MWNTs have much better conductivity than SWNTs, the quantitative difference in our S-parameter measurements of samples with and without MWNTs is much larger than in the SWNT measurements (when considering the number of SWNTs used in [16]).

Various factors may contribute to the resistance reduction of MWNTs with increasing frequency, which is very different from metal interconnects [19]. In the MWNTs, initially only the outermost shell directly contacting the electrode participates in the conduction. Then the number of conducting shells increases as the input frequency increases, which leads to the resistance reduction. In addition, the mean free path in metallic CNTs is much larger than in conventional metal, and the current density is much higher. More theoretical studies are required to validate this conjecture. In addition, to elucidate the contribution of contact resistance and substrate effects, more experiments using individual MWNTs of varying length are necessary.

5. Conclusion

In this paper, the RF characteristics of individual MWNTs were investigated for potential applications in nanoelectronic systems. Analysing distributed parameters of on-chip interconnects or transmission lines including frequency-dependent behaviour is essential for developing high-performance integrated systems. Experimental data were provided for the two-port S-parameter measurements from 0.5 to 50 GHz, and transmission parameters (R, L, G, and C) were extracted. Dynamic conductance, or the AC signal transmission capability of MWNTs, increases significantly as the frequency increases. Series resistance, inductance, and capacitance all decrease with increasing frequency, and dielectric loss increases. To the author's knowledge, this is the first experimental result that supports the frequency dependence of MWNT impedance at very high frequencies. Our findings demonstrate that MWNTs are promising for transmission lines or electronic interconnectors over a very wide frequency range. There remain many theoretical issues to understand the transmission mechanism of CNTs in the microwave frequency regime, and this study provides significant insight to further investigate the electric performance of MWNTs for a wider range of applications.

Acknowledgment

This work was supported in part by grant UD060037AD, administered via the Institute of Advanced Aerospace Technology at Seoul National University.

References

[1] Kong J, Soh H T, Cassell A, Quate C F and Dai H 1998 *Nature* **395** 878
[2] Bachtold A, Hadley P, Nakanishi T and Dekker C 2001 *Science* **294** 1317
[3] Rosenblatt S, Lin H, Sazonova V, Tiwari S and McEuen P 2005 *Appl. Phys. Lett.* **87** 15311
[4] Burke P J 2003 *IEEE Trans. Nanotechnol.* **2** 55
[5] Burke P J 2002 *IEEE Trans. Nanotechnol.* **1** 129
[6] Burke P J 2004 *Solid-State Electron.* **48** 1981
[7] Li S, Yu Z, Yen S F, Tang W C and Burke P J 2004 *Nano Lett.* **4** 753
[8] Yu Z, Rutherglen C and Burke P J 2006 *Appl. Phys. Lett.* **88** 233115
[9] Safi I and Schulz H J 1995 *Phys. Rev.* B **52** 17040
[10] Buttiker M and Christen T 1997 *Mesoscopic Electron Transport* 345 (Dordrecht: Kluwer) p 259
[11] Cuniberti G, Sassetti M and Kramer B J 1996 *J. Phys.: Condens. Matter* **8** 21
[12] Cuniberti G, Sassetti M and Kramer B J 1998 *Phys. Rev.* B **57** 1515
[13] Aronov I E, Beletskii N N, Berman G P, Campbell D K, Doolen G D and Dudiy S V 1998 *Phys. Rev.* B **58** 9894
[14] Yu Z and Burke P J 2005 *Nano Lett.* **5** 1403
[15] Zhao Y P, Wei B Q, Ajayan P M, Ramanath G, Lu T M, Wang G C, Rubio A and Roche S 2001 *Phys. Rev.* B **64** 201402
[16] Zhang M, Huo X and Chan P C H 2006 *Appl. Phys. Lett.* **88** 163109
[17] Tsutsui M, Kuno K, Kurokawa S and Sakai A 2007 *e-J. Surf. Sci. Nanotech.* **5** 12
[18] Dworsky L N 1979 *Modern Transmision Line Theory and Applications* (New York: Wiley)
[19] Eisenstadt W R and Eo Y 1992 *IEEE Trans. Compon. Hybrids Manuf. Technol.* **15** 483
[20] Pozar D M 2004 *Microwave Engineering* 3rd edn (New York: Wiley)
[21] Steinhogl W, Schindler G, Steinlesberger G and Engelhardt M 2002 *Phys. Rev.* B **66** 075414
[22] Ymeri H, Nauwelaers B and Maex K 2001 *J. Micromech. Microeng.* **11** 283